Dynamic modeling and control of a 4 DOF robotic finger using adaptive-robust and adaptive-neural controllers

F. Katibeh[a], M. Eghtesad[b,*] and Y. Bazargan-Lari[c]

[a] Ph.D Student of Mechanical Engineering, Shiraz University, Shiraz, Iran.
[b] School of Mechanical Engineering, Shiraz University, Shiraz, Iran.
[c] Department of Mechanical Engineering, Shiraz Branch, Islamic Azad University, Shiraz, Iran

ARTICLE INFO

ABSTRACT

In this research, first, kinematic and dynamic equations of a 4-DOF 3-link robotic finger are derived using Denavit-Hartenberg convention and Lagrange's formulation. To model the muscles, several springs and dampers are placed between the finger links. Then, two advanced controllers, namely adaptive-robust and adaptive-neural, which can control the robotic finger in presence of parametric uncertainty, are applied to the dynamic model of the system in order to track the desired trajectory of tapping. The simulation of the dynamic system is performed in presence of 10% uncertainty in the parameters of the system and the results are obtained when applying the two controllers separately on the robotic finger dynamic model. By comparing the simulation results of the tracking errors, it is observed that both controllers perform decently; however, the adaptive-neural controller has a better performance.

1. Introduction

In order to design robotic hands with dexterous activities, it is common, to take advantage of the inspirations of the human hand. Virtual reality (VR) and tele-operation are two prominent examples of using ideas of hand motion in the technology, [1]. Large number of DOFs of human hand makes it possible to orient it in arbitrary spatial positions and perform tasks like tapping, grasping, holding objects, etc. However, the large number of DOFs will make the study of hand's kinematics and dynamics very complicated. One way to overcome this difficulty is to, first, study a finger and then combine several fingers to complete biomechanical study of a hand.

In many researches, fingers are considered as three mechanical links attached together serially by revolute joints. In these researches that the methacarpophalangeal (MCP) joint is assumed as a 1 DOF hinge, the finger movements are assumed to be planar. A more complex finger has also been investigated assuming three dimensional 4-DOF motion of a digit [1]; in this research the second approach will be followed.

On the other hand, the hand muscles cause the hand motion to be soft and flexible and provide the ability to carry out precise jobs which need high excessive force. In recent biomechanical studies of human hand, some musculoskeletal models, an acknowledged one is the Hill's model, are used to find forces in the muscles, [2]. However, some other researchers have been trying to use new ways for modeling the muscles. Lee et al. investigated human upper extremity musculoskeletal structure by using adjustable springs to model the muscles, [3]. In this paper, the latter will be utilized. It is

Corresponding address: School of Mechanical Engineering, Shiraz University, Shiraz, Fars, Iran,
Tel.: +98 71 32303051; fax: +98 71 36287508. E-mail address fkatibe@gmail.com

a common practice for the researchers to employ the analytical methodologies to obtain robot dynamics; the most utilized ones are Newton and Lagrange's methods. For example, Boughdiri et al. derived an efficient dynamic equation for a multi fingered robot hand by the Lagrange's formulation [4]. The dynamic models can later be modified by using some experimental data, [5]. For example, Yun et al. analyzed repetitive finger flexion and extension by taking the measurement data from the CyberGlove system to obtain dynamic characteristics of the finger movement, [6].

The control problem of finger robots, and consequently multi fingered robot hands, is one of the challenging issues in this field due to highly nonlinear dynamic equations, external disturbances and parametric uncertainty. Mainly hand robots are controlled by either model based [7-9] or knowledge based [9-14] controllers. Model based controllers are usually used in the cases that high precision of fingertip position is needed. Therefore, the prerequisite of using these controllers is existence of a mathematical dynamic model for the system that can describe the robot behavior precisely, [6]. Boughdiri considers the problem of model-based control for a multi-fingered robot hand grasping an object with known geometrical characteristics [14].

In the article by Lee et al., a forward dynamic model of human multi-fingered hand movement is proposed. It is shown that if a simple PD control scheme is applied to the multi-link system, the resulting movements would be of different characteristics from those of actual human movements, [13]. Arimoto et al. utilized an intelligent controller for grasping and manipulation of an object performed by a multi-fingered robotic hand [15]. Lee et al. investigated finger joint coordination during tapping, using muscle activation patterns and energy profile [16]
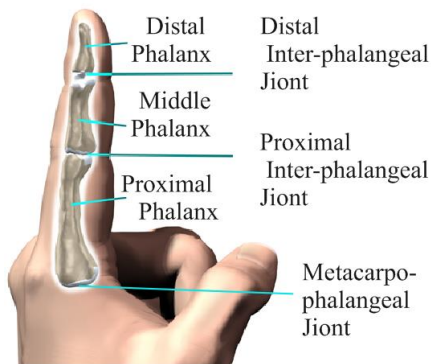

Figure 1. the schematic of the bone segments and joints of the index finger

A keystroke structure contains two basic movements: first, touching the key and pressing it downward; second, moving up the finger and releasing the keyswitch. While striking a key, the methacarpophalangeal joint flexes and the distal interphalangeal and proximal interphalangeal joints extend. During releasing a key the joints move in opposite direction to prepare for the next keystroke, [16]. The bone segments and joints of the index finger are shown in figure1.

In the current study, we attempt to obtain a human inspired model for one finger that includes the effects of muscles. After deriving a dynamic model by Lagrange's formulation for finger motion, we will try to apply two advanced controllers for tapping motion on a keyboard. The desired trajectory for tapping is extracted from the experimental data of finger joints, [2], and will be used as the reference input to the system.

2. Kinematics of the robotic finger

A 4 DOF serial robot is considered as the model of a finger robot. The first 2 DOFs correspond to the flexion-extension and abduction-adduction movements of the methacarpophalangeal joint. The third and fourth degrees of freedom are related to flexion-extension movements of proximal interphalangeal and distal interphalangeal joints, respectively. The muscles are simulated by setting some springs and dampers between the links. Lee et al. suggested an efficient way to put optimum number of springs between the links of a 3 DOF serial robot so the individual effect of each spring can be observed at the task space, [3]. As it is shown in Figure 2, six springs and dampers are located between the links which include three mono-articular, two bi-articular and one tri-articular springs.
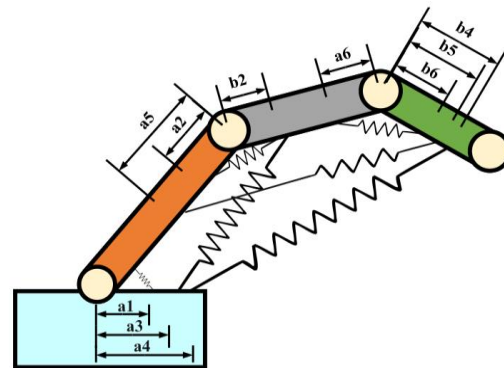

Figure 2. 2D schematic of finger robot and the location of spring-damper sets

As it can be seen in Figure 1, a_i and b_i, $i=$ 1, 2... 6, show the distances between the points that springs and dampers are attached to the links and joints. To obtain the kinematics and dynamics of a serial robot, the Denavit-Hartenberg convention is used to determine the required parameters for obtaining the homogenous transfer functions. The Denavit-Hartenberg parameters for each link can be determined as presented in Tabl1.

Table 1. The Denavit-Hartenberg parameters for each link of the finger robot

Link	d_i	a_i	α_i	θ_i
1	0	0	$\pi/2$	θ_1
2	0	L_2	$-\pi/2$	θ_2
3	0	L_3	0	θ_3
4	0	L_4	0	θ_4

L_i is the length of the segment of the link which is located between the joints i and $i + 1$. All the joints are revolute; so, the general coordinate q_i is defined as θ_i, the ith joint coordinate.

Using Denavit-Hartenberg convention and the related parameters (see Table 1), the homogeneous transformation matrix $^{i-1}A_i$ for each link can be obtained. The product of these matrices gives the matrix T_4 as follows:

In the forward kinematic problem the coordinates of the end-effector are obtained in terms of joint variables. The transformation matrix from the origin of the end-effector to the base reference frame is

$$
^{R}T_E = \begin{pmatrix}
c_\alpha \cdot c_\beta & c_\alpha \cdot s_\beta \cdot s_\gamma - s_\alpha \cdot c_\gamma & c_\alpha \cdot s_\beta \cdot c_\gamma + s_\alpha \cdot s_\gamma & x \\
s_\alpha \cdot c_\beta & s_\alpha \cdot s_\beta \cdot s_\gamma + c_\alpha \cdot c_\gamma & s_\alpha \cdot s_\beta \cdot c_\gamma - c_\alpha \cdot s_\gamma & y \\
-s_\beta & c_\beta \cdot s_\gamma & c_\beta \cdot c_\gamma & z \\
0 & 0 & 0 & 1
\end{pmatrix} \tag{1}
$$

The results of equating these two matrices are

$$
x = L_2 c_1 c_2 - L_4 s_4 (c_3 s_1 + c_1 c_2 s_3) - L_3 s_1 s_3 - L_4 c_4 (s_1 s_3 - c_1 c_2 c_3) + L_3 c_1 c_2 c_3 \tag{2}
$$

$$
y = L_4 s_4 (c_1 c_3 - c_2 s_1 s_3) + L_2 c_2 s_1 + L_3 c_1 s_3 + L_4 c_4 (c_1 s_3 + c_2 c_3 s_1) + L_3 c_2 c_3 s_1 \tag{3}
$$

$$
z = L_2 s_2 + L_3 c_3 s_2 + L_4 c_3 c_4 s_2 - L_4 s_2 s_3 s_4 \tag{4}
$$

Equations (3) to (5) give the position coordinates of the end-effector in the base frame. In order to obtain the roll-pitch-yaw angles of orientation of the end-effector with respect to the base frame, namely γ, β and α, we use the components 31, 32, 33, 21 and 11 of T_4 which yield

$$
\gamma = A\tan\left(\frac{-c_3 s_2 s_4 - c_4 s_2 s_3}{c_2}\right) \tag{5}
$$

$$
\beta = A\tan\left(\frac{-(c_3 c_4 s_2 - s_2 s_3 s_4),}{\frac{-c_3 s_2 s_4 - c_4 s_2 s_3}{s_\gamma}}\right) \tag{6}
$$

$$
\alpha = A\tan
$$
$$
\left(\begin{array}{c}
\dfrac{c_4(c_1 s_3 + c_2 c_3 s_1) + s_4(c_1 c_3 - c_2 s_1 s_3)}{c_\beta}, \\
\dfrac{-c_4(s_1 s_3 - c_1 c_2 c_3) - s_4(c_3 s_1 + c_1 c_2 s_3)}{s_\beta}
\end{array}\right) \tag{7}
$$

Where s_i stands for $\sin(\theta_i)$ and c_i sands for $\cos(\theta_i)$, $I = 1,\ldots, 4$. For the forward kinematics of the robot two sets of solution are obtained. The correct solution is chosen in a way that the end-effector coordinates change continuously.

3. Dynamics of the finger robot

There are two main approaches to generate the dynamic model of a robotic finger; Lagrange's formulation and Newton-Euler formulation. In this paper Lagrangian methodology is exploited to obtain the dynamic model of a robotic finger.

$$
T_4 = {}^0A_1 \, {}^1A_2 \, {}^2A_3 \, {}^3A_4 \tag{8}
$$

Applying Lagrange's formulation to a manipulator, results in a matrix form equation which is more appropriate for computer analysis [4].

The Extended Lagrange's equation when there exists dissipation energy is

$$
\frac{d}{dt}\left(\frac{\partial L}{\partial \dot{q}_i}\right) - \frac{\partial L}{\partial q_i} + \frac{\partial Q_f}{\partial \dot{q}_i} = \tau_i, \\
i = 1,2,\ldots,4 \tag{1}
$$

where, L is the Lagrangian function that is equal to the difference between the total kinetic energy, K, and the total potential energy, P; q_i is the ith generalized coordinate of the robot, $\dot{q}_i$ is the first time derivative of the corresponding generalized coordinate, Q_f is the dissipation energy of the system which is determined by calculating the dissipation energy in the dampers and τ_i is the generalized force (or torque) applied to the system at joint i to drive the ith link.

There are some major assumptions adopted in this study:

* Each finger is considered as a rigid body.

* Deformation of the fingertips is not considered.

* The finger segments are considered as the collection of cylindrical links.

Now we need to calculate the required energies to be substituted in Lagrange's formulation.

The kinetic energy for a 4 DOF serial robot is obtained by

$$K_i = \frac{1}{2} trace[\sum_{j=1}^{4}\sum_{k=1}^{4} \frac{\partial T_i}{\partial q_j} I_i \frac{\partial T_i^T}{\partial q_k} \dot{q}_j \dot{q}_k] \qquad (2)$$

Having the link transformation matrices, the homogenous transformation matrix from frame (i) to (0) is

$$T_i = {}^0A_1 \, {}^1A_2 \dots {}^{i-1}A_i \qquad (3)$$

As the links are assumed cylindrical, the matrix of moments of inertia will be obtained as:

$$I_i = \begin{bmatrix} \frac{1}{12}m_i L(i)^2 +m_i \overline{X}_i(1)^2 & 0 & 0 & m_i \overline{X}_i(1) \\ 0 & 0 & 0 & m_i \overline{X}_i(2) \\ 0 & 0 & 0 & m_i \overline{X}_i(3) \\ m_i \overline{X}_i(1) & m_i \overline{X}_i(2) & m_i \overline{X}_i(3) & 1 \end{bmatrix} \qquad (4)$$

where $\overline{X}_i$ is the center of gravity of the ith link and m_i is the total mass of the ith link. Then, the kinetic energy of each link can be obtained. The kinetic energy of the whole system is the summation of the kinetic energies of all links.

$$K = \sum_{i=1}^{4} K_i \qquad (5)$$

The potential energy in this study is due to elastic energy of the springs together with the gravitational energy of the links. The gravitational energy of each link can be computed as

$$P_g{}^i = -g^T T_i I_i e_4 \qquad (6)$$

where, T_i is the homogenous transformation matrix from frame (i) to (0), I_i is the matrix of moments of inertia of the ith link, the vector g is $g = \begin{bmatrix} g_x & g_y & g_z & 1 \end{bmatrix}^T$ and vector e_4 is defined as $e_4 = \begin{bmatrix} 0 & 0 & 0 & 1 \end{bmatrix}^T$.

The gravitational energy of the whole system is the summation of the gravitational energies of all links.

$$P_g = \sum_{i=1}^{4} P_g^i \qquad (7)$$

The next step is to calculate the elastic energy of each spring. The lengths of springs in an arbitrary position can be obtained according to the angles of orientations of the links. The number of the springs are defined as shown in Figure 3:
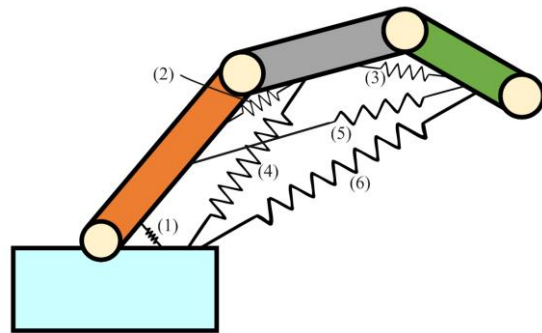

Figure 3. The number of the springs acting on the robotic finger

$$d_1 = \sqrt{a_1^2 + b_1^2 - 2a_1 b_1 \cos\theta_1}$$

$$d_2 = \sqrt{a_2^2 + b_2^2 - 2a_2 b_2 \cos\theta_3}$$

$$d_3 = \sqrt{\begin{array}{l}(l_1 - b_3\cos\theta_3 + a_3\cos\theta_1)^2 \\ +(-a_3\sin\theta_1 - b_3\sin\theta_3)^2\end{array}}$$

$$d_4 = \left(\begin{array}{l}\left(\begin{array}{l}l_1\cos\theta_1 + l_2\cos(\theta_1+\theta_3) \\ +b_6\cos(\theta_1+\theta_3+\theta_4)\end{array}\right)^2 \\ +\left(\begin{array}{l}l_1\sin\theta_1 \\ +l_2\sin(\theta_1+\theta_3) \\ +b_6\sin(\theta_1+\theta_3+\theta_4)\end{array}\right)^2\end{array}\right)^{.5} \qquad (8)$$

$$d_5 = \sqrt{\begin{array}{l}(l_2 - a_5\cos\theta_3 - b_5\cos\theta_4)^2 \\ +(-b_5\sin\theta_4 + a_5\sin\theta_3)^2\end{array}}$$

$$d_6 = \sqrt{a_6^2 + b_6^2 - 2a_6 b_6 \cos\theta_4}$$

The elastic energy of spring i is then

$$P_e^i = \frac{1}{2}K_{ki}(d_i - d_i^0)^2 \quad i = 1,2,\dots,6 \qquad (9)$$

Where K_{ki} and d_i^0 are the stiffness coefficient and the initial length of spring i, respectively.

The total elastic energy of the robot is the summation of elastic energies of all 6 springs.

$$P_e = \sum_{i=1}^{6} P_e^i \qquad (10)$$

Now the total potential energy of the finger robot is calculated by adding total elastic energy and total gravitational energy of the system as

$$P_T(q) = P_g + P_e \tag{11}$$

In order to calculate the dissipation energy of each damper, it is required to obtain the rate of length change of each damper. So, the dissipation energy of each damper can be obtained as

$$Q_i = \frac{1}{2} C_i \dot{d}_i^2 \tag{12}$$

Where C_i and $\dot{d}_i$ represent damping ratio and rate of length change of damper i, respectively.

Total dissipation energy of the finger robot is the summation of dissipation energies of all dampers.

$$Q(q, \dot{q}) = \sum_{i=1}^{6} Q_i \tag{13}$$

Having the kinetic and potential energies of the system, the Lagrangian L is defined as

$$L(q, \dot{q}) = K(q, \dot{q}) - P(q) \tag{14}$$

After substituting the corresponding terms of system energies in the Lagrangian's formulation, the dynamic of one finger digit is described by the following

$$M(q)\ddot{q} + C(q, \dot{q})\dot{q} + G(q) = \tau \tag{15}$$

Where M is the matrix of inertia, each of its components can be calculated as

$$m_{ij} = \sum_{k=\max(i,j)}^{4} trace(\frac{\partial T_k}{\partial q_j} I_k \frac{\partial T_k^T}{\partial q_j}) \tag{16}$$

C consists of Coriolis, centrifugal and gyroscopic terms and each of its components can be obtained as

$$c_{ij} = \sum_{k=1}^{4} \left(\frac{1}{2} \frac{\partial M_{jk}}{\partial q_i} + \frac{1}{2} \frac{\partial M_{ik}}{\partial q_j} - \frac{1}{2} \frac{\partial M_{ij}}{\partial q_k} \right) \dot{q}_k \tag{17}$$

Matrices M and C are the same in both skeletal and musculoskeletal models of a digit.

G is obtained by differentiating the total potential energy with respect to the vector of generalized coordinates, q:

$$G = \frac{\partial P_T(q)}{\partial q} \tag{18}$$

The vector F which indicates the damping terms is calculated as:

$$F = \frac{\partial Q(q, \dot{q})}{\partial \dot{q}} \tag{19}$$

After determining the elements of matrices it can be shown the matrix $N = \dot{M} - 2C$ is skew-symmetric.

4. Control of the robotic finger

So far, we have derived the dynamic equations of a finger robot (containing the effects of muscles by considering some springs and dampers in the system). Now, it is possible to apply any model based controllers to the system in addition to intelligent controllers.

The coefficients of springs and dampers are not constant and vary in a specific range based on the movement of the finger. These coefficient variations in the dynamic model cause uncertainties in the model of the system. The adaptive-robust and adaptive-neural control methods considered in this research can add robustness to the control system against these uncertainties.

In the following, the tracking of the desired trajectory of tapping is investigated considering 10% uncertainties in the values of masses, stiffness parameters of springs and coefficients of dampers while the mentioned controllers are applied to the system.

5. Adaptive-Robust control method

The combination of robust and adaptive controllers has some prominence over each of them alone. This combination makes the control system overcome each controller's disadvantages and show good performance in the presence of disturbances and parameter uncertainties.

In this research, first, based on a robust control method, some bounds are assumed on the parameters and then by using the adaptive method these bounds are estimated.

The control law then would be as chosen as equations (20), (22)

$$\tau = \hat{M}\ddot{\varsigma} + \hat{C}\dot{\varsigma} + \hat{g} - K_D \sigma + u_0 \tag{20}$$

$$\dot{\varsigma} = \dot{q}_d - \Lambda \tilde{q} \tag{21}$$

Where $\tilde{q} = q - q_d$

$$\sigma = \dot{q} - \dot{\varsigma} = \dot{\tilde{q}} + \Lambda \tilde{q} \tag{22}$$

In which $\hat{M}, \hat{C}$ and $\hat{G}$ are approximations of M, C and G. K_D and Λ are positive definite matrices and q_d represents the vector the desired trajectories of the generalized coordinates.

We can rewrite equation (20) as

$$M\dot{\sigma} + C\sigma + K_D = \tilde{w} + u_0 \tag{23}$$

Where

$$\tilde{w} = (\hat{M} - M)\ddot{\varsigma} + (\hat{C} - C)\dot{\varsigma} + (\hat{g} - g) \tag{24}$$

u_0 can then be taken as

$$u_0 = -(\rho^2/(\varepsilon + \rho\|\sigma\|))\sigma \qquad (25)$$

Where ρ is defined as

$$\begin{aligned}\rho &= \delta_0 + \delta_1\|e\| + \delta_2\|e\|^2 \\ &= [1 \quad \|e\| \quad \|e\|^2][\delta_0 \quad \delta_1 \quad \delta_2]^T = S\theta\end{aligned} \qquad (26)$$

Where $e = [\tilde{q} \; \dot{\tilde{q}}]$.

The vector of estimated parameters θ will be updated by

$$\dot{\hat{\theta}} = \dot{\tilde{\theta}} = -\gamma S^T\|\sigma\| \qquad (27)$$

Where $\tilde{\theta} = \hat{\theta} - \theta$ and they are defined as

$$\hat{\rho} = S\hat{\theta} \, , \tilde{\rho} = S\tilde{\theta} \qquad (28)$$

with $\|\tilde{w}\| \le \rho$.

And the time derivative of ε can be defined as

$$\dot{\varepsilon} = -k_\varepsilon \varepsilon, \varepsilon(0) > 0 \qquad (29)$$

where K_ε is selected as a positive definite matrix. Figure 4 shows the schematic of the closed-loop control system when applying the adaptive-robust controller.
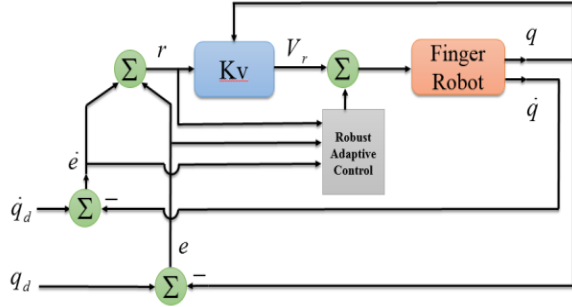
Figure 4. The schematic of the adaptive-robust controller

By taking the Lyapanov function as

$$V = \frac{1}{2}\sigma^T M\sigma + \frac{1}{2}\tilde{\theta}^T\gamma^{-1}\tilde{\theta} + K_\varepsilon^{-1}\varepsilon \qquad (30)$$

It can be shown that its time derivative is

$$\begin{aligned}\dot{V} &= \frac{1}{2}\sigma^T\dot{M}\sigma + \sigma^T M\dot{\sigma} + \tilde{\theta}^T\gamma^{-1}\dot{\tilde{\theta}} \\ &\quad + K_\varepsilon^{-1}\dot{\varepsilon}\end{aligned} \qquad (31)$$

By substituting equations (23) and (27) in (39), we will have:

$$\begin{aligned}\dot{V} &= \frac{1}{2}\sigma^T\dot{M}\sigma + \sigma^T(w' - C\sigma - K_D\sigma + u_0) \\ &\quad + \tilde{\theta}^T\gamma^{-1}(-\gamma S^T\|\sigma\|) \\ &\quad + K_\varepsilon^{-1}(-K_\varepsilon\varepsilon)\end{aligned} \qquad (32)$$

Using skew-symmetric property of $\dot{M} - 2C$ and substituting equations (25), (26), (28) and (29), we can rewrite equation (40) as:

$$\begin{aligned}\dot{V} &= \sigma^T w' + \sigma^T u_0 - \sigma^T K_D\sigma - \tilde{\theta}^T S^T\|\sigma\| \\ &\quad - \varepsilon \\ &\le \sigma^T\rho + \sigma^T u_0 - \sigma^T K_D\sigma - \tilde{\theta}^T S^T\|\sigma\| \\ &\quad - \varepsilon \\ &\le \hat{\theta}^T S^T\|\sigma\| - \sigma^T\sigma\frac{\hat{\rho}^2}{\varepsilon + \hat{\rho}\|\sigma\|} - \sigma^T K_D\sigma \\ &\quad - \varepsilon \\ &\le \frac{-\varepsilon S\hat{\theta}\|\sigma\| - \varepsilon^2 + \varepsilon S\hat{\theta}\|\sigma\|}{\varepsilon + S\hat{\theta}\|\sigma\|} - \sigma^T K_D\sigma \\ &= -\frac{\varepsilon^2}{\varepsilon + S\hat{\theta}\|\sigma\|} - \sigma^T K_D\sigma \le -\sigma^T K_D\sigma\end{aligned} \qquad (33)$$

By using Barbalat lemma and the fact that $\dot{V}$ is negative definite, considering equation (33), it can be proved that the vector of tracking error asymptotically approaches zero.

6. Adaptive-Neural control method

A neural network is usually used to approximate the dynamic model of a system. Based on the offline data taken from the system, an appropriate controller is applied to the system which causes the system to be compatible with the changes occurring in it. As a result, the combination of neural network and adaptive controller could be considered as a suitable control method for the systems with uncertainties in model parameters. In the following, the adaptive-neural control method is applied to the finger robot considering uncertainties in the parameters of the system. In this method a three layer Gaussian radial basis function neural network is used to parametrize the control law. (An identification law then identifies the parameters of the neural network and at the end the stability of the closed-loop system is guaranteed by the Lyapanov method).

The Gaussian function is shown in eqation (34)

$$a_i(y) = \exp(-\frac{(y - \mu_i)^T(y - \mu_i)}{\sigma^2}) \qquad (34)$$

The static neural network of $M(q)$ and $G(q)$ which are just functions of q would be as considered as equations (35) and (36)

$$M(q) = [\{\Theta\}^T \bullet \{\Xi(q)\}] + E_D(q) \qquad (35)$$

$$G(q) = [\{B\}^T \bullet \{H(q)\}] + E_G(q) \qquad (36)$$

and the dynamic neural network of $C(q,\dot{q})$ which is function of both q and $\dot{q}$ will be as

$$C(q,\dot{q}) = [\{A\}^T \bullet \{Z(z)\}] + E_C(z) \qquad (37)$$

Let $q_d(t)$ be the desired trajectory in the joint space and $\dot{q}_d(t)$ and $\ddot{q}_d(t)$ be the desired velocity and acceleration. Defining

$$e(t) = q_d(t) - q(t) \qquad (38)$$

$$\dot{q}_r(t) = \dot{q}_d(t) + \Lambda e(t) \qquad (39)$$

$$r(t) = \dot{q}_r(t) - \dot{q}(t) = \dot{e}(t) + \Lambda e(t) \qquad (40)$$

where Λ is a positive definite matrix. It can be easily shown that if $\lim_{t\to\infty} r = 0$, then $\lim_{t\to\infty} e = 0$. The control law then would be chosen as equation (41).

$$\tau = \left[\{\hat{\Theta}\}^T \bullet \{\Xi(q)\}\right]\ddot{q}_r + \left[\{\hat{A}\}^T \bullet \{Z(z)\}\right]\dot{q}_r + \left[\{\hat{B}\}^T \bullet \{H(q)\}\right] + K_r r + K_s sgn(r) \qquad (41)$$

where $K \in R^{n \times n}$ and $K_s > \|E\|$, with $E = E_D(q)\ddot{q}_r + E_c(z)\dot{q}_r + E_G(q) + \tau_f(\dot{q})$. The first three terms of the control law are model-based control terms, whereas the K_r term gives the proportional derivative (PD) type of control. The last term in the control law is added to suppress the modeling errors of the neural networks. Figure 5 shows the schematic of the neural adaptive control system.
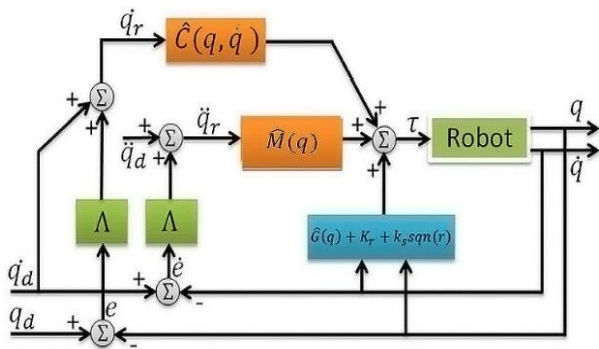
Figure 5. The schematic of neural adaptive control system

Consider the nonnegative scalar function V as

$$V = \frac{1}{2}r^T M(q)r + \frac{1}{2}\sum_{k=1}^{n} \tilde{\theta}_k{}^T \Gamma_k^{-1}\tilde{\theta}_k + \frac{1}{2}\sum_{k=1}^{n} \tilde{\alpha}_k{}^T Q_k^{-1}\tilde{\alpha}_k + \frac{1}{2}\sum_{k=1}^{n} \tilde{\beta}_k{}^T N_k^{-1}\tilde{\beta}_k \qquad (42)$$

to be the Lyapunov candidate, where Γ_k, N_k and Q_k are dimensional compatible symmetric positive-definite matrices. Computing the derivative of equation (42) and simplifying it yield

$$\dot{V} = r^T(M(q)\dot{r} + C(q,\dot{q})r) + \sum_{k=1}^{n} \tilde{\theta}_k{}^T \Gamma_k^{-1}\dot{\tilde{\theta}}_k + \sum_{k=1}^{n} \tilde{\alpha}_k{}^T Q_k^{-1}\dot{\tilde{\alpha}}_k + \sum_{k=1}^{n} \tilde{\beta}_k{}^T N_k^{-1}\dot{\tilde{\beta}}_k \qquad (43)$$

Where the property of skew-symmetric has been used. In order to make the time derivative of the Lyapunov function be negative-definite, the update law for the weight parameters should be chosen as

$$\dot{\hat{\theta}} = \Gamma_k \bullet \{\xi_k(q)\}\ddot{q}_r r_k$$

$$\dot{\hat{\alpha}} = Q_k \bullet \{\zeta_k(z)\}\dot{q}_r r_k \qquad (44)$$

$$\dot{\hat{\beta}} = N_k \eta_k(q) r_k$$

Substituting the weight parameter update laws into Equation (43), with $K_s > \|E\|$ yields

$$\dot{V} \leq -r^T K_r r \leq 0 \qquad (45)$$

Therefore, $\lim_{t\to\infty} r = 0$, and so, it can be proved that the vector of tracking error, e, asymptotically approaches zero.

7. Simulation and Results

The finger robot studied in this research is a four DOF robot that all of its joints are revolute. One actuator is located on each single joint (total of four actuators) to provide the required torques computed by the controller to obtain the desired motion. The act of controlling is computerized using Simulink toolbox of MATLAB. The desired values of the joint angles are extracted from the experimental research done by Kuo et al., [2]. The act of tapping happens at 0.35 seconds and contains a full motion from striking the keyboard till rising the finger up. The values of the desired joint coordinates *vs.* time are given in Figure 6.
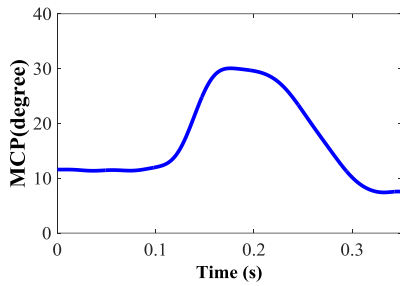
A
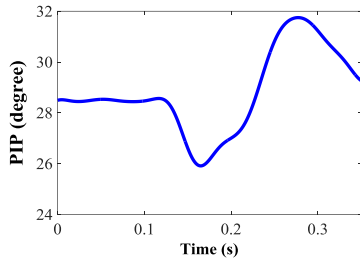
b
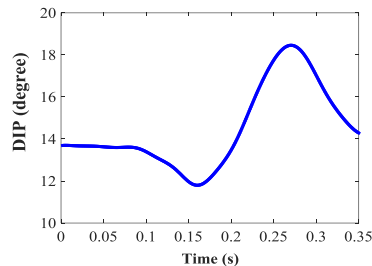
c

Figure 6. The desired angles of joints: (a) methacarpophalangeal, (b) proximal interphalangeal (c) distal interphalangeal during tapping

The desired motion of tapping is considered inside the plane so the desired motion of the 2nd DOF in methacarpophalangeal joint is set to the amount of zero.

In the following the results of simulation of the finger robot when adaptive-robust and adaptive-neural controllers are applied to the dynamical system are shown. The results contain the variations of the generalized coordinates, θ_i, s, (actual and desired) versus time and the tracking error for each DOF.

The initial values of joints angles are set as $q^0 = \begin{Bmatrix} 0.1 \\ 0 \\ 0.3 \\ 0.1 \end{Bmatrix}$.

First the results of finger robot when applying the adaptive-robust controller are studied. The parameters of the control law are set as $K_D = 10\, I_{20 \times 20}$, $\gamma = 0.8$, $K_\varepsilon = 0.1$.

Figure 7 illustrates the actual angles of joints compared with the desired path of tapping after applying the robust adaptive controller to the finger robot.
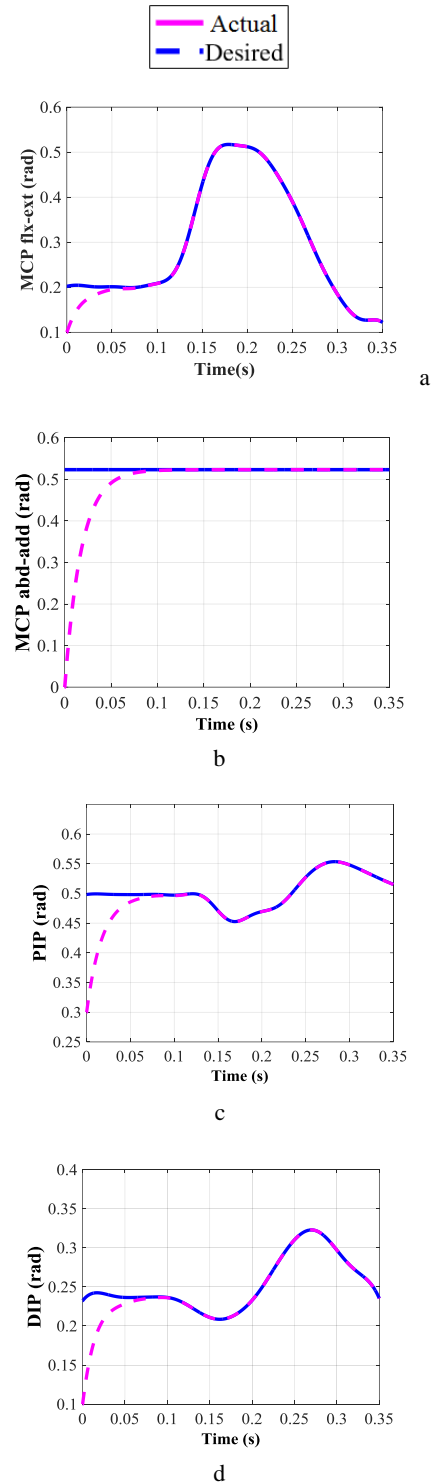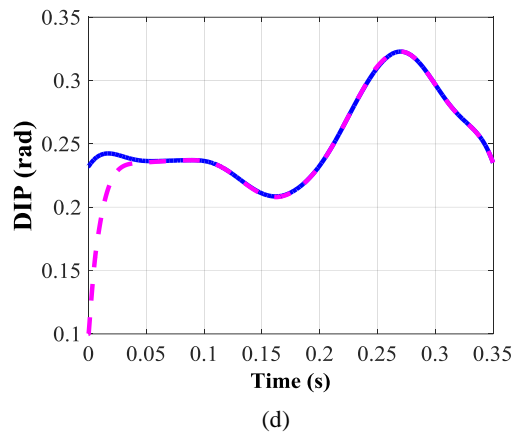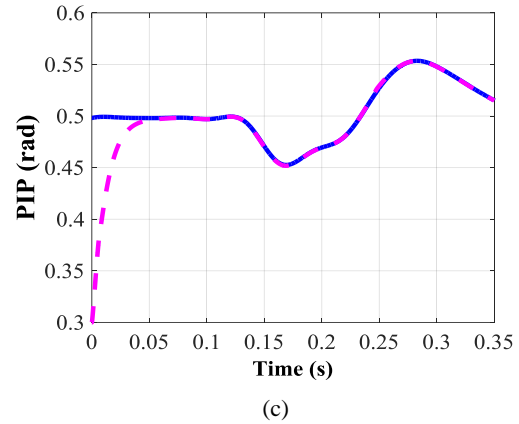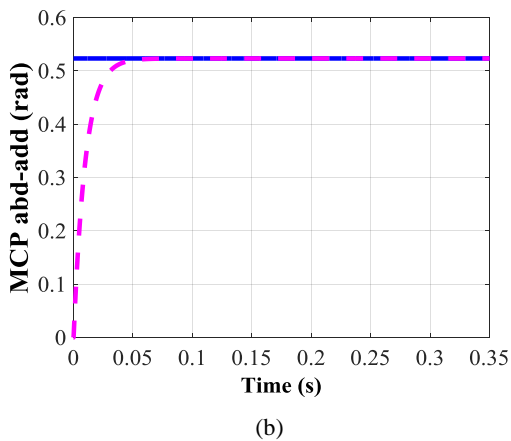

a

b

c

d

Figure 7. The actual angles of (a) methacarpophalangeal flexsion-extension, (b) methacarpophalangeal abduction-adduction, (c) Proximal interphalangeal (d) distal interphalangeal joints versus the desired path of tapping after applying the robust adaptive controller on the finger robo*t*

As it is shown in the figures, each individual joint tracks the corresponding desired trajectory properly. Next, the results of adaptive-neural controller are shown. The parameters of the control law are set to

$$K_r = 10^2. \begin{bmatrix} 1000 \\ 0100 \\ 0010 \\ 0001 \end{bmatrix} \quad , \quad K_s = 0.1.$$

Figure 8 illustrates the actual angles of joints compared with the desired path of tapping after applying the neural adaptive controller to the finger robot.
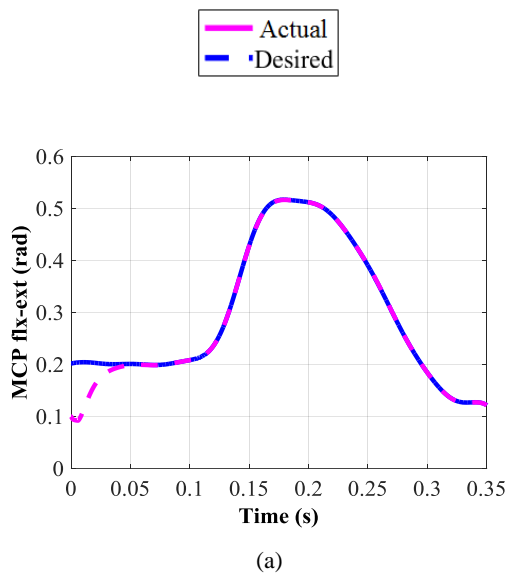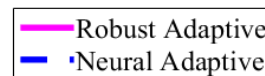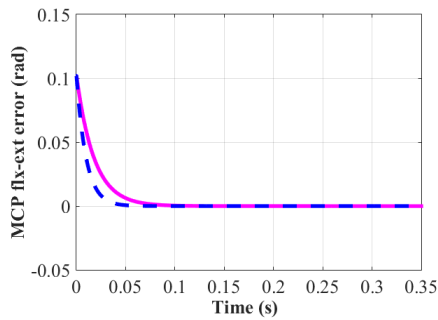

(a)

(b)

(c)

(d)

Figure 8. The actual angles of (a) methacarpophalangeal flexsion-extension, (b) methacarpophalangeal abduction-adduction, (c) Proximal interphalangeal (d) distal interphalangeal joints versus the desired path of tapping after applying the neural adaptive controller on the finger robot
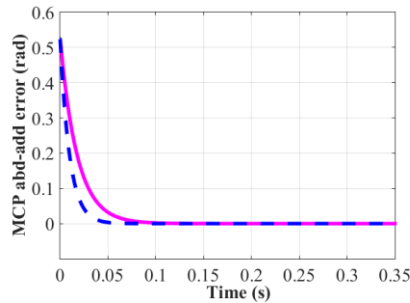
As it is shown in the figures, each individual joint tracks its corresponding desired trajectory properly.

Now the tracking errors of the generalized coordinates under application of either controller are illustrated and compared in Figure 9.
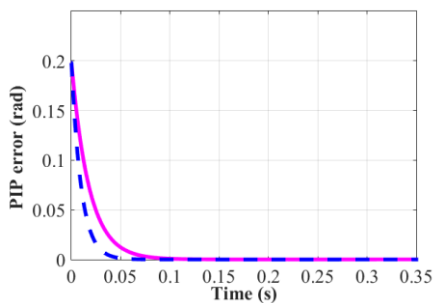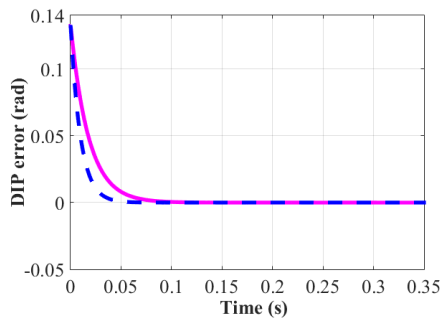
(a)

(b)

(c)

(d)

Figure 9. The error of (a) methacarpophalangeal flexsion-extension, (b) methacarpophalangeal abduction-adduction, (c) Proximal interphalangeal (d) distal interphalangeal joints from the desired values after applying robust adaptive and neural adaptive controllers on the finger robot.

As it is shown in the figures the adaptive-neural controller can make the error vanish in less time than the robust adaptive. Based on the figures it is observed that both of the proposed controllers are able to make the joint angles follow the desired trajectory properly despite the 10% uncertainties in the system parameters. However under the application of the intelligent control method- neural adaptive controller- reaching the desired convergence happens at a lower time (14% of total time) than the robust adaptive controller (19% of total time).

8. Conclusion

Considering the model offered for the human upper-extremity by Lee et al. [3] a new musculoskeletal model for a robotic finger has been studied.

The model was assumed as a 3-D one; but, the considered motion in this paper, tapping, was a 2-D one. The dynamic equations derived based on Lagrange's formulation. Then adaptive-robust and adaptive-neural controllers are applied to the system and the procedure has been computerized using Simulink toolbox of MATLAB. Based on the results it is observed that the model is validated. Also, by comparing the 2 controllers it can be resulted that the neural adaptive controller has a better performance.

As future works, it is aimed to model and control the 5-finger robotic hand in order to do the tasks like holding and grasping an object.

References

[1]   J. Sancho-Bru, A. Perez-Gonzalez, M. Vergara-Monedero, and D. Giurintano, A 3-D dynamic model of human finger for studying free movements, Journal of biomechanics, Vol. 34, (2001) 1491-1500.

[2]   C. Huang, B. Li, S. Xiao, and R. Wang, A forward musculoskeletal dynamics approach to the motion of metacarpophalangeal joint of index finger, Engineering in Medicine and Biology Society, Proceedings of the 20th Annual International Conference of IEEE, (1998) 2486-2489.

[3]   J. H. Lee, B.-J. Yi, and J. Y. Lee, Adjustable spring mechanisms inspired by human musculoskeletal structure," Mechanism and Machine Theory, Vol. 54, (2012) 76-98.

[4]   R. Boughdiri, H. Bezine, N. Sirdi, A. Naamane and A. M. Alimi, Dynamic modeling of a multi-fingered robot hand in free motion, 8th International Multi-Conference on Systems, Signals and Devices (SSD), (2011) 1-7.

[5]   S. Bae and T. J. Armstrong, A finger motion model for reach and grasp, International journal of industrial ergonomics, Vol. 41, (2011) 79-89.

[6] M. H. Yun, H. J. Eoh, and J. Cho, A two-dimensional dynamic finger modeling for the analysis of repetitive finger flexion and extension, International Journal of Industrial Ergonomics, Vol. 29, (2002) 231-248.

[7] Z. Doulgeri and J. Fasoulas, Grasping control of rolling manipulations with deformable fingertips, Mechatronics, IEEE/ASME Transactions on, Vol. 8, (2003) 283-286.

[8] S. Ueki, H. Kawasaki, and T. Mouri, Adaptive coordinated control of multi-fingered hands with sliding contact, International Joint Conference, SICE-ICASE, (2006) 5893-5898.

[9] Z. Doulgeri and Y. Karayiannidis, Force position control for a robot finger with a soft tip and kinematic uncertainties, Robotics and Autonomous Systems, Vol. 55, (2007) 328-336.

[10] E. Al-Gallaf, Neurofuzzy inverse Jacobian mapping for multi-finger robot hand control, Journal of Intelligent and Robotic Systems, Vol. 39, (2004) 17-42.

[11] G. Wöhlke, A neuro-fuzzy-based system architecture for the intelligent control of multi-finger robot hands, in Fuzzy Systems, Proceedings of the Third IEEE World Congress on Computational Intelligence, (1994) 64-69.

[12] H. Liu, T. Iberall and G. A. Bekey, Neural network architecture for robot hand control, Control Systems Magazine, IEEE, Vol. 9, (1989) 38-43.

[13] S.-W. Lee and X. Zhang, Biodynamic modeling, system identification, and variability of multi-finger movements, Journal of biomechanics, Vol. 40, (2007) 3215-3222.

[14] R. Boughdiri, H. Nasser, H. Bezine, N. K. M'Sirdi, A. M. Alimi, and A. Naamane, Dynamic modeling and control of a multi-fingered robot hand for grasping task, Procedia Engineering, Vol. 41, (2012) 923-931.

[15] S. Arimoto, Intelligent control of multi-fingered hands, Annual Reviews in Control, Vol. 28, (2004) 75-85.

[16] P.-L. Kuo, D. L. Lee, D. L. Jindrich and J. T. Dennerlein, Finger joint coordination during tapping, Journal of biomechanics, Vol. 39, (2006) 2934-2942.

[17] F. L. Lewis, C. T. Abdallah and D. M. Dawson, Control of robot manipulators, Macmillan, New York, Vol. 236, (1993).

[18] S. Jung and T. Hsia, Neural network impedance force control of robot manipulator, Industrial Electronics, IEEE Transactions on, Vol. 45, (1998) 451-461.

Biography

Fatemeh Katibeh is currently a Ph.D. student in Mechanical Engineering Department, Shiraz University. She received her BSc. and MSc. degrees in mechanical engineering from Shiraz University in 2011, 2014 respectively. Her research interests include Biomechanics, Robotics and control.

Mohammad Eghtesad received his B.Sc. from university of Tehran (1983), M.Sc. from University of Tehran (1987) and Ph.D. from University of Ottawa (1996). He joined the School of Mechanical Engineering at Shiraz University in 1997 where he is currently a full Professor. He has taught and done research in the area of robotics, mechatronics and control. His research includes both theoretical and experimental studies. Since 2012 he is the editor-in-chief of Iranian Journal of Science and Technology, Transactions of Mechanical Engineering.

Yousef Bazargan Lari is an assistant Professor in the Department of Mechanical Engineering at the Shiraz Branch of Islamic Azad University where he has been a faculty member since 2009. He is a member of American Society of Mechanical Engineering. He completed his PhD at Science and Research Branch of Islamic Azad University He also finished his undergraduate study at Shiraz University in 2006. His research interests lie in advanced dynamics and control.